DOI: 10.17725/rensit.2023.15.441

Evaluation of noise immunity of multi-user mimo systems with imperfect channel estimation and other distortions

Artem Shinkevich, Dmitry A. Pokamestov, Yakov V. Kryukov, Evgeny V. Rogozhnikov, Georgy N. Shalin, Andrey A. Brovkin

Tomsk State University of Control Systems and Radioelectronics, https://tusur.ru/
Tomsk 634050, Russian Federation

E-mail: a.shinkevich00@gmail.com, dmaltomsk@mail.ru, kryukov.tusur@gmail.com, udzhon@mail.ru, shalingn1120@gmail.com, soldierbrovkin@gmail.com

Received August 09, 2023, peer-reviewed August 16, 2023, accepted August 23, 2023, published December 06, 2023.

Abstract: **The technology of multi-antenna MIMO (Multiple Input Multiple Output) systems is actively used in modern wireless communication systems. MIMO can enhance the performance of wireless data transmission systems, but their effectiveness depends on the transmission conditions. Ideal conditions are represented as a channel with a large number of possible signal propagation paths and an error-free estimation of its parameters. The estimation error significantly affects the performance of the beamforming algorithms used to mitigate inter-user interference in multi-user MIMO (MU-MIMO) systems. Spatial correlation of the channel results in a decrease in the number of independent information transmission streams. These factors can significantly reduce the performance of multi-antenna systems. For this reason, operating MIMO communication systems under non-ideal conditions is a topical issue. The paper examines the performance of various beamforming algorithms in such conditions. It describes the communication systems with MIMO, beamforming algorithms, and distorting effects. The paper includes a developed simulation model of the communication channel with MU-MIMO accounting for a variety of distorting factors. The results demonstrate the bit-error probability dependences for different simulation scenarios**

Keywords: **MIMO, MU-MIMO, gigital precoding, hybrid beamforming, imperfect CSI, Los channel, spatial correlation**

UDC 621.396.4

Acknowledgments: The research was carried out at the expense of the grant of the Russian Science Foundation No. 22-79-10148, https://rscf.ru/project/22-79-10148/.

For citation: Artem Shinkevich, Dmitry A. Pokamestov, Yakov V. Kryukov, Evgeny V. Rogozhnikov, Georgy N. Shalin, Andrey A. Brovkin. Evaluation of noise immunity of multi-user mimo systems with imperfect channel estimation and other distortions. *RENSIT: Radioelectronics. Nanosystems. Information Technologies*, 2023, 15(4):441-452e. DOI: 10.17725/rensit.2023.15.441.

Contents

1. **Introduction (441)**
2. **Beamforming in MU-MIMO (443)**
   - 2.1. **Block Diagonalization (444)**
   - 2.2. **Dirty-Paper Coding (444)**
   - 2.3. **Tomlinson-Harashima (445)**
   - 2.4. **Channel Inversion (446)**
   - 2.5. **Hybrid Beamforming (446)**
3. **Simulation results (447)**
4. **Conclusion (450)**

References (451)

1. INTRODUCTION

Wireless communication systems are widely used nowadays. The growing transmitted

data volumes and the development of new applications led to increased demands for modern communication systems: spectral and energy efficiency, data rate, noise immunity, mitigation of delays, the ability to connect a large number of subscribers, etc.

Multi-antenna Multiple Input Multiple Output (MIMO) systems are one of the key technologies for increasing spectral efficiency, and, accordingly, data rate and noise immunity of the transmission. Unlike traditional single-antenna Single Input Single Output (SISO) systems, MIMO uses multiple antennas both on the transmitting and receiving sides. Ideally for systems with MIMO, the number of independent streams is a multiple of the number of antennas. This is achieved in an uncorrelated multipath channel with non-line-of-sight, where the receiver is synchronous with the transmitter and ideally evaluates the frequency response (FR) of the channel. However, in real systems, due to the physical proximity of antenna elements, there is a spatial correlation of signals, and noise does not allow for an accurate assessment of the channel frequency response. Some scenarios are characterized by the line of sight, which also leads to signal correlation. These factors significantly affect the MIMO performance, impairing the efficiency of multiplexing and channel noise immunity.

There are two types of MIMO: single-user (SU-MIMO) and multi-user (MU-MIMO). In multi-user systems, a base station with multiple antennas can simultaneously transmit a signal to several subscriber stations with one or more antennas (broadcast channel) [1]. It is also possible that many subscribers with one or more antennas transmit a signal to one base station with several antennas (multiple access channel) [1].

Inter-user interference, caused by signals intended for other subscribers, should be mitigated. Different types of beamforming are used to tackle this issue with MU-MIMO systems making it possible to perform this procedure in a digital, analog or hybrid (digital and analog) form.

Analog beamforming, which originated in the middle of the 20th century, is directly related to phased arrays. In modern systems employing analog beamforming, signals from the radio frequency (RF) circuit are fed to phase shifters before reaching the antenna elements, which allows for real-time adjustments to the antenna pattern [2].

In the case of digital beamforming, the signal from the modulator output arrives at a digital preliminary coder (precoder), where it is multiplied by the calculated coefficients. This operation results in changing both the signal amplitude and its phase. There are different precoding algorithms, for example, Block Diagonalization (BD) [3], Channel Inversion (ChI) [4], Dirty-Paper Coding (DPC) [5], Tomlinson–Harashima (TH) [6], and others [7–8].

Hybrid beamforming combines analog beamforming and digital precoding. In this case, signal is processed in the time and frequency domain. Currently, hybrid beamforming is the main technology for massive MIMO (mMIMO) systems, as well as communication systems in the mmWave range [9].

Even though the algorithms used in MU-MIMO have been known for a long time, the evaluation and comparison of various beamforming methods are poorly represented in the literature. This article addresses the impact of various distorting factors on the signal noise immunity, including frequency response estimation errors, spatial correlation, and Rice *K*-factor,

when using different beamforming methods. It also describes the obtained dependences of the bit error probabilities and the ratio of energy per bit of information to spectral power density of noise. There are conclusions about the effectiveness and applicability of the considered methods presented.

2. BEAMFORMING IN MU-MIMO

Fig. 1 shows the structural schemes of systems employing different variants of beamforming. For digital and hybrid adaptive beamforming on the transmitting side, it is required to have the channel state information (CSI), which is transmitted via the feedback channel. In real systems, the presence of noise often hinders the accurate estimation of the channel parameters. The CSI discreteness also affects the performance of MIMO systems, underscoring the need to take into account the imperfection of the estimation when considering the effectiveness of beamforming algorithms.

As the problem statement, let us consider a mathematical model of the MU-MIMO system with digital beamforming (precoding). Its block diagram is presented in **Fig. 2**.

Let $\mathbf{s}^1$, …, $\mathbf{s}^K$ be the modulation symbols of K subscribers. $\mathbf{S}=\left[\left(\mathbf{s}^1\right)^{\mathrm{T}},\cdots,\left(\mathbf{s}^k\right)^{\mathrm{T}}\right]^{\mathrm{T}}$, — the transposition operation, $\mathbf{V}_1$, …, $\mathbf{V}_K$ are

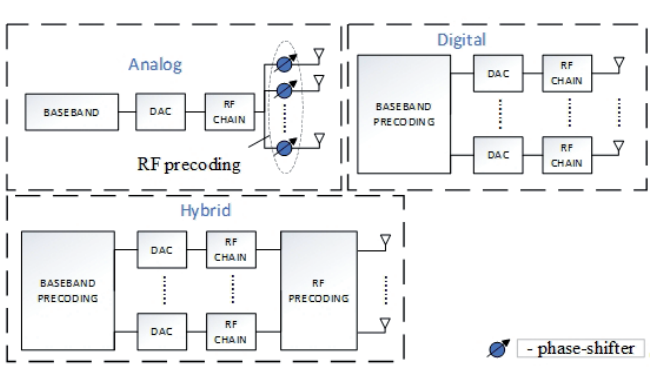

Fig. 1. *Beamforming types.*

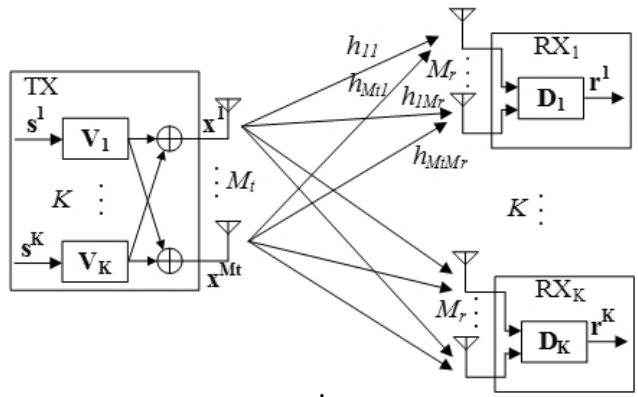

Fig. 2. *Block diagram of MU-MIMO system with precoding.*

precoding matrices. $\mathbf{V}=\left[\mathbf{V}_1,\cdots,\mathbf{V}_K\right]$, $\mathbf{x}^{\mathrm{k}}$ are symbol vectors transmitted through M_{t} antennas,

$$\mathbf{X}=\left[\left(\mathbf{x}^1\right)^{\mathrm{T}},\cdots,\left(\mathbf{x}^k\right)^{\mathrm{T}}\right]^{\mathrm{T}},$$

$$\mathbf{X}=\mathbf{VS}=\sum_{k=1}^{K}\mathbf{x}^k=\sum_{k=1}^{K}\mathbf{V}_k\mathbf{s}^k.$$

Let $\mathbf{y}^{\mathrm{k}}$ represent the signal sample vector at the input of the kth receiver, and $\mathbf{n}^{\mathrm{k}}$ represent the sample vector of noise implementations at the input of the kth receiver; $\mathbf{H}_{\mathrm{k}}$ is the matrix of channel coefficients for the kth receiver, $\mathbf{H}=\left[\mathbf{H}_1{}^{\mathrm{T}},\ldots,\mathbf{H}_K{}^{\mathrm{T}}\right]^{\mathrm{T}}$.

$$\mathbf{y}^k=\mathbf{H}_k\mathbf{X}+\mathbf{n}^k=\mathbf{H}_k\mathbf{x}^k+\sum_{i=1,i\neq k}^{K}\mathbf{H}_k\mathbf{x}^i+\mathbf{n}^k=$$

$$=\mathbf{H}_k\mathbf{V}_k\mathbf{s}^k+\sum_{i=1,i\neq k}^{K}\mathbf{H}_k\mathbf{V}_i\mathbf{s}^i+\mathbf{n}^k,$$

$$\mathbf{Y}=\mathbf{HX}+\mathbf{N},$$

$$\mathbf{N}=\begin{bmatrix}\mathbf{n}^1\\ \vdots\\ \mathbf{n}^K\end{bmatrix}=\begin{bmatrix}n_1\\ \vdots\\ n_{KMr}\end{bmatrix}.$$

In each of the K receivers, the signal is postprocessed using matrices $\mathbf{D}_{\mathrm{k}}$, and the reconstructed signal for the kth user $\mathbf{r}^{\mathrm{k}}$ is described by the following expressions:

$$\mathbf{r}^k=\mathbf{D}_k\mathbf{y}^k,$$

$$\mathbf{r}^k=\mathbf{D}_k\left(\mathbf{H}_k\mathbf{V}_k\mathbf{s}^k+\sum_{i=1,i\neq k}^{K}\mathbf{H}_k\mathbf{V}_i\mathbf{s}^i+\mathbf{n}^k\right).$$

Thus, $\mathbf{D}_k\mathbf{H}_k\mathbf{V}_k\mathbf{s}^k$ is a desired signal intended for the *k*th subscriber, and $\sum_{i=1,i\neq k}^{K}\mathbf{D}_k\mathbf{H}_k\mathbf{V}_i\mathbf{s}^i$ is an interference component.

The problem of digital beamforming can be formulated as the problem of mitigating the interference component, which is equivalent to the expression:

$$\sum_{i=1,i\neq k}^{K}\mathbf{D}_k\mathbf{H}_k\mathbf{V}_i\mathbf{s}^i \equiv \mathbf{\Theta},$$

where $\mathbf{\Theta}$ is the zero vector.

Therefore, the problem is reduced to finding precoding matrices $\mathbf{V}_i$ and postprocessing matrices $\mathbf{D}_k$.

Let us examine the precoding types mentioned earlier, along with the hybrid beamforming.

2.1. Block Diagonalization

To form a precoding matrix for the *k*th user, it is required to have information about the status of channels of other users, that is, the interference matrix, which includes channel matrices between the base station and other users [3]:

$$\hat{\mathbf{H}}_k = \left[\hat{\mathbf{H}}_1^{\mathrm{T}},\cdots,\hat{\mathbf{H}}_{k-1}^{\mathrm{T}},,\hat{\mathbf{H}}_{k+1}^{\mathrm{T}}\cdots\hat{\mathbf{H}}_k^{\mathrm{T}}\right]^{\mathrm{T}}. \quad (1)$$

After that, the singular value decomposition (SVD) of the resulting matrix is performed and the matrix rank is calculated:

$$\hat{L}_k = \mathrm{rank}\left(\hat{\mathbf{H}}_k\right),$$

$$\hat{\mathbf{H}}_k = \hat{\mathbf{U}}_k\hat{\mathbf{\Lambda}}_k\left[\hat{\mathbf{V}}_k^{(1)}\hat{\mathbf{V}}_k^{(0)}\right]^{\mathrm{H}},$$

where $\mathbf{U}_k$ are left singular vectors; $\mathbf{\Lambda}_k$ is a diagonal matrix containing the singular numbers of matrix $\mathbf{H}_k$; $\mathbf{V}_k^{(1)}$ are the first L_k of the right singular vectors of matrix $\mathbf{V}_k$; $\mathbf{V}_k^{(0)}$ are $(N_{tx} - L_k)$ of the right singular vectors of matrix $\mathbf{V}_k$; and $\mathbf{V}_k^{(0)}$ forms an orthogonal basis for the space of (1) [3]. And in what follows, $(\bullet)^{\mathrm{H}}$ is the Hermitian transpose.

The next step is to perform SVD of the product of the channel matrix for the kth user and $\hat{\mathbf{V}}_k^{(0)}$:

$$\mathbf{H}_k\hat{\mathbf{V}}_k^{(0)} = \mathbf{U}\mathbf{\Lambda}\left[\mathbf{V}_k^{(1)}\mathbf{V}_k^{(0)}\right]^{\mathrm{H}}.$$

As a result, the general precoding matrix can be represented as: $\mathbf{V} = \left[\hat{\mathbf{V}}_1^{(0)}\mathbf{V}_1^{(1)},\hat{\mathbf{V}}_2^{(0)}\mathbf{V}_2^{(1)},\ldots,\hat{\mathbf{V}}_K^{(0)}\mathbf{V}_K^{(1)}\right]$.

The postprocessing matrix can be expressed as follows [3]:

$$\mathbf{D} = \begin{bmatrix} \mathbf{U}_1^{\mathrm{H}} & \cdots & \mathbf{0} \\ \vdots & \ddots & \vdots \\ \mathbf{0} & \cdots & \mathbf{U}_K^{\mathrm{H}} \end{bmatrix}.$$

2.2. Dirty-Paper Coding

The DPC algorithm is based on an *LQ* decomposition of the channel matrix [1], which is, in turn, associated with a *QR* decomposition:

$$\mathbf{H} = \mathbf{L}\mathbf{Q}, \quad (2)$$

where $\mathbf{L}$ is a lower triangular matrix (with elements above the main diagonal being zero), and $\mathbf{Q}$ is the orthogonal matrix ($\mathbf{Q}\mathbf{Q}^{\mathrm{H}} = \mathbf{Q}^{\mathrm{H}}\cdot\mathrm{Q} = \mathbf{I}$).

$$\mathbf{H} = \mathbf{Q}\mathbf{R}, \quad (3)$$

where $\mathbf{R}$ is an upper triangular matrix (with elements below the main diagonal being zero), and $\mathbf{Q}$ is the orthogonal matrix.

Let us derive the relation of the *LQ* and *QR* decompositions (2) and (3):

$$(\mathbf{Q}\mathbf{R})^{\mathrm{H}} = \mathbf{R}^{\mathrm{H}}\mathbf{Q}^{\mathrm{H}} = \mathbf{L}\mathbf{Q}^{\mathrm{H}} = \mathbf{H}^{\mathrm{H}}. \quad (4)$$

From equation (4), it follows that the *QR* decomposition of matrix $\mathbf{H}^{\mathrm{H}}$ will be the Hermitian-transposed *LQ* decomposition of matrix $\mathbf{H}$.

The precoding matrix is calculated based on matrix $\mathbf{L}$. Multiplying the precoded signal by $\mathbf{Q}^{\mathrm{H}}$ eliminates the impact of $\mathbf{Q}$ [1]. Considering this, the received signal can be written as follows [1]:

$$\mathbf{Y} = \mathbf{HQ}^{\mathrm{H}}\mathbf{X} + \mathbf{Z} = \mathbf{LQQ}^{\mathrm{H}}\mathbf{X} + \mathbf{Z} = \\ = \mathbf{LX} + \mathbf{Z} = \begin{pmatrix} l_{11} & 0 & \cdots & 0 \\ l_{21} & l_{22} & \cdots & 0 \\ \vdots & \vdots & \ddots & \vdots \\ l_{m1} & l_{m2} & \cdots & l_{mm} \end{pmatrix} \begin{pmatrix} x_1 \\ x_2 \\ \vdots \\ x_m \end{pmatrix} + \begin{pmatrix} z_1 \\ z_2 \\ \vdots \\ z_m \end{pmatrix}, \quad (5)$$

where $\mathbf{X}$ is the precoded signal and $\mathbf{Z}$ is the noise.

Let us express the reception conditions without interference from (5).

For the first antenna, it is expressed as:

$$x_1 = \tilde{x}_1, \quad (6)$$

where $\tilde{x}_1$ is the signal at the precoder input.

From (5), the condition for the 2nd antenna can be expressed as:

$$x_2 = \tilde{x}_2 - \frac{l_{21}}{l_{22}} x_1, \quad (7)$$

from equations (6) and (7), the condition for the ith antenna is represented as:

$$x_i = \tilde{x}_i + \sum_{k=1}^{i-1} (-1) \frac{l_{ik}}{l_{ii}} x_k.$$

Therefore, the precoding matrix can be described using the following expression [1]:

$$\begin{pmatrix} 1 & 0 & \cdots & 0 \\ -\frac{l_{21}}{l_{22}} & 1 & \cdots & 0 \\ \vdots & \vdots & \ddots & \vdots \\ -\frac{l_{m1}}{l_{mm}} & -\frac{l_{m2}}{l_{mm}} & \cdots & 1 \end{pmatrix} = \\ = \begin{pmatrix} l_{11} & 0 & \cdots & 0 \\ l_{21} & l_{22} & \cdots & 0 \\ \vdots & \vdots & \ddots & \vdots \\ l_{m1} & l_{m2} & \cdots & l_{mm} \end{pmatrix}^{-1} \begin{pmatrix} l_{11} & 0 & \cdots & 0 \\ 0 & l_{12} & \cdots & 0 \\ \vdots & \vdots & \ddots & \vdots \\ 0 & 0 & \cdots & l_{mm} \end{pmatrix}. \quad (8)$$

The precoded signal can be expressed using the following formula:

$$\mathbf{X} = \mathbf{L}^{-1} \operatorname{diag}(\mathbf{L}) \tilde{\mathbf{X}}, \quad (9)$$

where $\mathbf{L}$ is the matrix resulting from the LQ decomposition of matrix $\mathbf{H}$, $\tilde{\mathbf{X}}$ is the signal from the output of the modulator, and *diag* are the elements of the main diagonal.

The postprocessing for this algorithm is expressed as follows [1]:

$$\hat{\mathbf{X}} = \begin{pmatrix} l_{11} & 0 & \cdots & 0 \\ 0 & l_{12} & \cdots & 0 \\ \vdots & \vdots & \ddots & \vdots \\ 0 & 0 & \cdots & l_{mm} \end{pmatrix}^{-1} \mathbf{Y}, \quad (10)$$

where $\hat{\mathbf{X}}$ is the reconstructed signal.

DPC is a non-linear algorithm enabling the maximum possible bandwidth in MIMO systems. However, this algorithm is of limited practical utility, due to its high computational complexity and the associated increase in transmission power caused by the algorithm peculiarities.

2.3. Tomlinson-Harashima

The TH algorithm can be considered as a variant of DPC with a symmetric modulo operation. Initially, TH was introduced to diminish peak or average power in the Decision Feedback Equalizer (DFE). The concept behind applying TH in DFE is to mitigate the impact of postcursor intersymbol interference (ISI) [10] on the transmitting side, where the transmitted symbols are known a priori [11,12].

Let us denote the signal precoded by the DPC algorithm (9) as $\mathbf{C}$.

The symmetric modulo operation for a signal can be expressed as follows:

$$\mathbf{X} = \mathbf{C} - 2A \left\lfloor \frac{(\mathbf{C} + A + jA)}{2A} \right\rfloor, \quad (11)$$

where $A = \sqrt{M}$, M is the modulation order, $\mathbf{X}$ is the precoded signal, and $\lfloor\ \rfloor$ is the operation of rounding down to the nearest integer.

Expression 11 can be transformed as follows:

$$\mathbf{X} = \mathbf{C} - 2A \left(\left\lfloor \frac{\mathrm{Re}(\mathbf{C}) + A}{2A} \right\rfloor + j \left\lfloor \frac{\mathrm{Im}(\mathbf{C}) + A}{2A} \right\rfloor \right), \quad (12)$$

where Re is the real part of the number, Im is the imaginary part of the number, and j denotes the imaginary unit.

The postprocessing problem is simplified to expression 10 from DPC and the subsequent modulo operation (12).

2.4. Channel Inversion

Precoding that uses the ChI algorithm for MU-MIMO systems essentially amounts to a pre-equalization operation [13] used in SU-MIMO systems, which is based on the same expressions.

In the case of zero-forcing (ZF), the precoding matrix is expressed as follows:

$$\mathbf{W}_{ZF} = \beta \mathbf{H}^{-1}, \quad (13)$$

where $\mathbf{H}$ is the channel matrix, β is the coefficient used to limit the total transmitted power after pre-equalization.

Coefficient β is calculated using the formula:

$$\beta = \sqrt{\frac{N_{TX}}{\mathrm{Tr}\left(\mathbf{H}^{-1}\left(\mathbf{H}^{-1}\right)^{H}\right)}},$$

where N_{TX} is the number of transmitting antennas, $\mathbf{H}$ is the channel matrix, and Tr is the matrix trace, that is, the sum of elements on the main diagonal.

This coefficient allows for normalizing the output power to 1 watt.

Postprocessing is simplified to dividing the received signal by β:

$$\hat{\mathbf{X}} = \frac{\mathbf{Y}}{\beta},$$

where $\mathbf{Y}$ is the received signal and $\hat{\mathbf{X}}$ is the reconstructed signal.

By definition, β is the gain factor for an automatic gain control (AGC) system.

In the case of the Minimum Mean Squared Error (MMSE) equalizer, equation (13) takes the following form:

$$\mathbf{W} = \beta \mathbf{H}^{H}\left(\mathbf{H}\mathbf{H}^{H} + \frac{N_{TX} \cdot 10^{\left(\frac{-SNR}{10}\right)}}{2}\mathbf{I}\right)^{-1},$$

where $\mathbf{I}$ is the identity matrix with ones on the main diagonal, and SNR is the signal-to-noise ratio measured in dB.

2.5. Hybrid Beamforming

Hybrid beamforming is a combined method that employs analog beamforming while using phase shifters. In numeric simulation, the analog beamforming matrix contains shift coefficients for each RF circuit. The digital precoding matrix, in turn, contains specific weights for signal processing in the frequency domain. This method allows combining the advantages of digital and analog beamforming to achieve the best performance with minimal complexity of equipment and energy consumption [14].

To calculate the precoding and postprocessing matrices, approximation is used, involving the decomposition of a signal into basic functions from a predefined set (codebook), where these functions are called atoms. Sparse approximation, in turn, aims to approximate the signal using the smallest number of elements, while maintaining the number of errors lower than a specified threshold level, i.e.

$$f(t) = \sum_{m=0}^{N-1} a_m g_m(t) + \mathbf{r}_N,$$
$$\|\mathbf{r}_N\| \to \min, \quad \|\mathbf{a}\|_0 \to \min,$$

where a_m is the decomposition coefficient; $g_m(t)$ is the codebook atom $\mathbf{D}$; N is the number of decomposition elements; $\mathbf{r}_N$ is the approximation error; $\|\bullet\|$ —the norm; and $\|\bullet\|_0$ is pseudonorm L_{-0}, equal to the number of non–zero elements of the vector.

The problem of determining digital ($\mathbf{F}_{bb}$) and analog ($\mathbf{F}_{rf}$) precoding matrices can be formulated as maximizing mutual

information, $\arg\max_{(\mathbf{F}_{rf},\mathbf{F}_{bb})}\left(\mathrm{I}\left(\mathbf{F}_{rf},\mathbf{F}_{bb}\right)\right)$, expressed by the following formula:

$$\mathrm{I}\left(\mathbf{F}_{rf},\mathbf{F}_{bb}\right)= \\ =\log_2\left(\det\left(\mathbf{I}+\frac{\rho}{N_s\sigma^2}\mathbf{H}\mathbf{F}_{rf}\mathbf{F}_{bb}\mathbf{F}_{bb}^{\mathrm{H}}\mathbf{F}_{rf}^{\mathrm{H}}\mathbf{H}^{\mathrm{H}}\right)\right). \quad (14)$$

At the same time, by using SVD and its properties [15], equation (14) can be transformed as follows:

$$\mathrm{I}\left(\mathbf{F}_{rf},\mathbf{F}_{bb}\right)= \\ =\log_2\left(\det\left(\mathbf{I}+\frac{\rho}{N_s\sigma^2}\mathbf{\Sigma}^2\,\mathbf{V}^{\mathrm{H}}\mathbf{F}_{rf}\mathbf{F}_{bb}\mathbf{F}_{bb}^{\mathrm{H}}\mathbf{F}_{rf}^{\mathrm{H}}\mathbf{V}\right)\right), \quad (15)$$

where $\mathbf{V}$ and $\mathbf{\Sigma}$ are the matrices from the singular decomposition of matrix $\mathbf{H}$; ρ is the average power of the transmitter; N_S is the number of digital streams; and σ^2 is the noise variance.

In addition, $\mathbf{V} = [\mathbf{V}_1\mathbf{V}_2]$. Through mathematical substitutions in (15), as elaborated in [16], the optimal precoding matrix is represented as $\mathbf{F}_{\mathrm{opt}}=\mathbf{V}_1$. Furthermore, based on these transformations, the problem of determining precoding matrices can be reformulated as follows:

$$\left[\mathbf{F}_{bb},\mathbf{F}_{rf}\right]=\arg\min_{(\mathbf{F}_{bb},\mathbf{F}_{rf})}\left(\left\|\mathbf{F}_{opt}-\mathbf{F}_{rf}\mathbf{F}_{bb}\right\|_{\mathrm{F}}\right), \quad (16)$$

where $\|\bullet\|_{\mathrm{F}}$ is the Frobenius norm.

The mathematical apparatus of sparse approximation is well-developed and highly suitable for calculating precoding and postprocessing matrices in the context of hybrid beamforming. In particular, equation (16) can be solved using the Orthogonal Matching Pursuit (OMP) algorithm [17]. Although there are other algorithms, for example, manifold optimization-based AltMin (MO-AltMin) [18], OMP offers significantly lower computational complexity with a slight decrease in spectral efficiency gain [19]. For this reason, this algorithm was used in the simulation.

The signal at the input of the receiving antenna can be recorded as follows:

$$\mathbf{y}=\mathbf{H}\mathbf{F}_{rf}\mathbf{F}_{bb}\mathbf{x}+\mathbf{n}.$$

The postprocessing problem is to minimize the Mean Squared Error (MSE) between the signal from the modulator output and the received signal after processing $\arg\min_{(\mathbf{W}_{rf},\mathbf{W}_{bb})}\left(\mathrm{E}\left\{\left\|\mathbf{x}-\mathbf{W}_{bb}^{\mathrm{H}}\mathbf{W}_{rf}^{\mathrm{H}}\mathbf{y}\right\|_2^2\right\}\right)$, hereafter, E{...} is the averaging operator.

Consequently, the optimal postprocessing matrix is the MMSE equalization matrix, which in this case can be expressed as follows:

$$\mathbf{W}_{MMSE}^{\mathrm{H}}=\mathrm{E}\left\{\mathbf{s}\mathbf{y}^{\mathrm{H}}\right\}\mathrm{E}\left\{\mathbf{y}\mathbf{y}^{\mathrm{H}}\right\}^{-1}= \\ =\frac{1}{\sqrt{\rho}}\left(\mathbf{F}_{bb}^{\mathrm{H}}\mathbf{F}_{rf}^{\mathrm{H}}\mathbf{H}^{\mathrm{H}}\mathbf{H}\mathbf{F}_{rf}\mathbf{F}_{bb}+\frac{\sigma^2N_s}{\rho}\mathbf{I}\right)^{-1}\mathbf{F}_{bb}^{\mathrm{H}}\mathbf{F}_{rf}^{\mathrm{H}}\mathbf{H}^{\mathrm{H}}. \quad (17)$$

Taking into account (17) and using transformations, the determination of digital and analog postprocessing matrices can be simplified to the following expression:

$$\left[\mathbf{W}_{rf},\mathbf{W}_{bb}\right]= \\ =\arg\min_{(\mathbf{W}_{rf},\mathbf{W}_{bb})}\left(\left\|\mathrm{E}\left\{\mathbf{y}\mathbf{y}^{\mathrm{H}}\right\}^{\frac{1}{2}}\left(\mathbf{W}_{MMSE}-\mathbf{W}_{rf}\mathbf{W}_{bb}\right)\right\|_{\mathrm{F}}\right).$$

The OMP algorithm [17] can also used to solve this problem.

The reconstructed signal can be written as follows:

$$\hat{\mathbf{x}}=\mathbf{W}_{bb}\mathbf{W}_{rf}\mathbf{y}.$$

3. SIMULATION RESULTS

To assess the noise immunity ensured by using different types of beamforming, a mathematical model of a broadcast MU-MIMO communication system has been developed. **Table 1** contains the main simulation parameters.

The simulation has been carried out under different scenarios. The results are the dependences of BER on E_0/N_0.

In the first scenario, the channel coefficients obey the Rayleigh distribution.

Table 1

Simulation parameters

Modulation	QPSK
Transmitting antennas number	16
Number of users	4
Number of receiving antennas per user	4
Message size	320 bits per user
Signal-to-noise ratio range	[0-30]
Iterations number	1000

The simulation in this scenario has been carried out for the BD, ChI, DPC, TH algorithms with perfect and imperfect CSI estimation.

Perfect estimation assumes that the transmitter knows the instantaneous values of the channel matrix. It is important to note that the channel is stationary, and CSI perfectly aligns with the channel matrix. Imperfect estimation implies the presence of noise due to which the receiver cannot accurately estimate both the channel and the temporary non-stationarity of the channel frequency response.

Fig. 3 shows the obtained dependences of the BER estimation on the ratio of the energy per bit of information to the noise power spectral density E_b/N_0 for different root-mean-square error (MSE) estimates.

The second scenario considers the influence of the line of sight on the noise immunity. The presence of line of sight impairs the performance of multi-antenna systems because it leads to a decrease in the channel matrix rank. Channel coefficients obey the Rice distribution. In this scenario, the channel matrix can be described by the following formula:

$$\mathbf{H} = \sqrt{\frac{K}{1+K}}\mathbf{H}_{LoS} + \sqrt{\frac{1}{1+K}}\mathbf{H}_{NLoS},$$

where $\mathbf{H}_{LoS}$ is the line-of-sight component, $\mathbf{H}_{NLoS}$ is a random component of the channel matrix, and K is the Rice factor (the ratio of the direct ray power to the power of the other rays).

The line-of-sight component can be represented as follows:

$$\mathbf{H}_{LoS} = \mathbf{a}_{rx}(\theta_{rx})\left(\mathbf{a}_{tx}(\theta_{tx})\right)^{\mathrm{T}},$$

where $\mathbf{a}_{\mathrm{rx}}(\theta_{\mathrm{rx}})$ and $\mathbf{a}_{\mathrm{tx}}(\theta_{\mathrm{tx}})$ are the responses of the receiving and transmitting antenna arrays, respectively; θ_{rx} and θ_{tx} are the receiving and transmitting angles, respectively.

Fig. 4 shows the obtained dependences of BER on E_b/N_0 at different values of the Rice coefficient K.

The K = 2 coefficient indicates a weak line of sight, K = 100 implies a weakly expressed multipath nature, K = 10 suggests the presence of both multipath and line-of-sight components.

The simulation for the third scenario has been performed in a correlated Rayleigh channel. In this scenario, the channel coefficients follow the Rayleigh distribution,

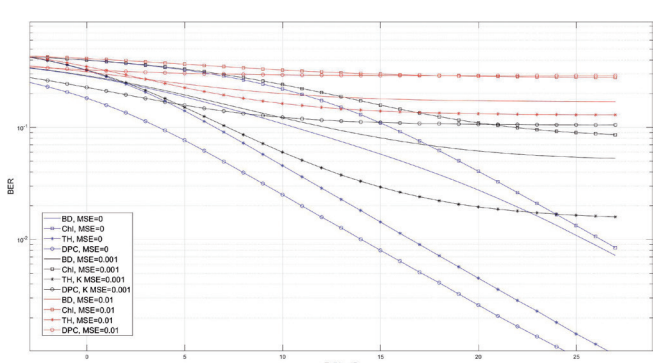

Fig. 3. *Dependences of BER on E_b/N_0 in the Rayleigh channel with different estimation errors*

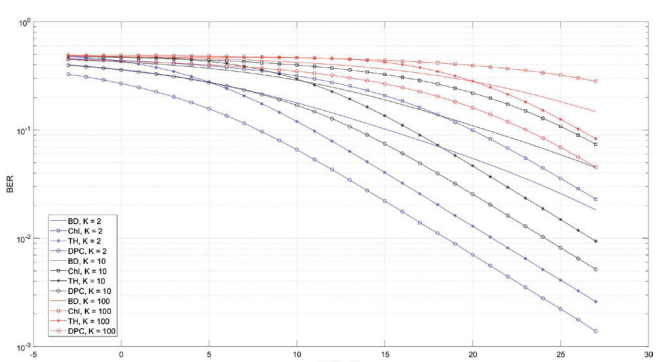

Fig. 4. *Dependences of BER on E_b/N_0 in the Rice channel with different values of coefficient K.*

but it is characterized by spatial correlation on both the receiving and transmitting sides caused by the physical proximity of antenna elements and the limited diversity of the propagation medium. Considering this, the channel matrix can be written as follows [1]:

$$\mathbf{H} = \mathbf{R}_{rx}^{1/2}\mathbf{H}_{\omega}\mathbf{R}_{tx}^{1/2},$$

where $\mathbf{R}_{rx}$, $\mathbf{R}_{tx}$ are the correlation matrices on the receiving and transmitting sides, respectively, and $\mathbf{H}_{\omega}$ is the uncorrelated channel matrix.

Correlation matrices take the following form:

$$\mathbf{R}_{tx} = \begin{bmatrix} 1 & \rho_{tx} & \rho_{tx}^4 & \cdots & \rho_{tx}^{(N-1)^2} \\ \rho_{tx} & 1 & \rho_{tx} & \cdots & \vdots \\ \rho_{tx}^4 & \rho_{tx} & 1 & \cdots & \rho_{tx}^4 \\ \vdots & \vdots & \vdots & \ddots & \rho_{tx} \\ \rho_{tx}^{(N-1)^2} & \cdots & \rho_{tx}^4 & \rho_{tx} & 1 \end{bmatrix},$$

$$\mathbf{R}_{rx}^k = \begin{bmatrix} 1 & \rho_{rx} & \rho_{rx}^4 & \cdots & \rho_{rx}^{(N-1)^2} \\ \rho_{rx} & 1 & \rho_{rx} & \cdots & \vdots \\ \rho_{rx}^4 & \rho_{rx} & 1 & \cdots & \rho_{rx}^4 \\ \vdots & \vdots & \vdots & \ddots & \rho_{rx} \\ \rho_{rx}^{(N-1)^2} & \cdots & \rho_{rx}^4 & \rho_{rx} & 1 \end{bmatrix},$$

$$\mathbf{R}_{rx} = \begin{bmatrix} \mathbf{R}_{rx}^1 & 0 & \cdots & 0 \\ 0 & \mathbf{R}_{rx}^2 & \cdots & 0 \\ \vdots & \vdots & \ddots & \vdots \\ 0 & 0 & \cdots & \mathbf{R}_{rx}^K \end{bmatrix},$$

where $\mathbf{R}_{rx}^k$ is the correlation matrix for the kth user, while ρ_{tx} and ρ_{rx} are the correlation coefficients on the transmitting and receiving sides. **Fig. 5** shows the obtained dependences.

The selection of these correlation coefficient values is justified as follows: when $\rho = 0.5$ is true, the correlation introduces minimal distortions, whereas when $\rho = 0.8$ holds true, the correlation already has a strong impact.

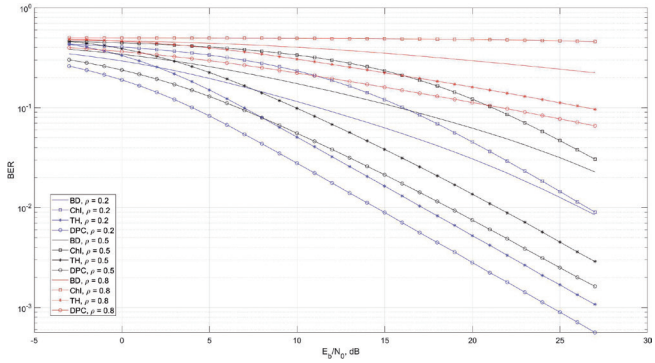

Fig. 5. *Dependences of BER on E_b/N_0 in the Rayleigh channel for various spatial correlation coefficient values*

The last scenario considers hybrid beamforming and takes into account the spatial separation of subscribers. Number of digital streams Ns = 4, the architecture is fully connected. Users are evenly distributed around the base station. The distance between BS and UEs is in the range of 200–4000 wavelengths, which corresponds to a distance of up to 570 meters at 1800 MHz and up to 200 meters at 6 GHz. Such coverage areas are common for small cells where MIMO technology is actively used. **Fig. 6** illustrates the obtained dependences for a different number of RF circuits (NTRF) on the transmitting side, considering both perfect and imperfect estimation of the channel matrix.

Figs 3–6 demonstrate that imperfect estimation, the presence of a line of sight, and the correlation contribute to a significant

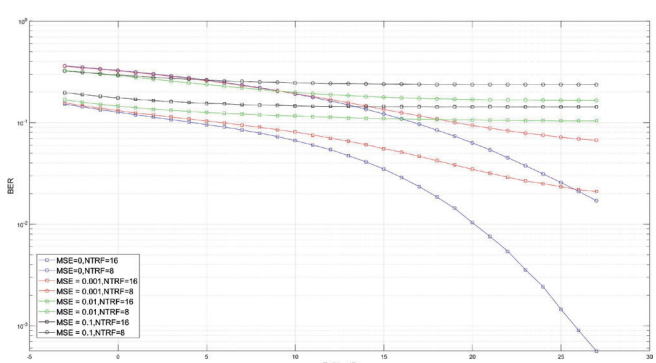

Fig. 6. *Dependences of BER on E_b/N_0 – for hybrid beamforming with varying estimation errors and different number of RF circuits.*

decrease in the noise immunity of MIMO systems.

Fig. 3 illustrates that among digital algorithms, DPC shows the best noise immunity performance, but only with perfect estimation. Even a small estimation error (MSE = 0.001) results in a sharp decrease in noise immunity, with BER > 0.1. The TH algorithm is behind the DPC algorithm in performance by about 2.5 dB (with perfect estimation), but it is less sensitive to estimation errors. Even with a small estimation error, the value of BER < 0.1 can be achieved via only TH or BD algorithms (BER is 0.02 and 0.06, respectively). With MSE = 0.01, none of the precoding algorithms can achieve a bit error probability of 0.1. With perfect estimation, the ChI algorithm is behind BD by about 1 dB in terms of BER = 0.01, but a small estimation error also leads to a significant decrease in noise immunity, with BER > 0.1.

For Figs 4, 5, the performance degradation is considered relative to the uncorrelated Rayleigh channel with perfect estimation. Fig. 4 shows that even a weak line of sight (K = 2) significantly diminishes the system noise immunity. At E_b/N_0 = 27 dB, BER increases by about 3 times for all types of precoding. At K = 10, BER increases by about 10 times for the DPC and TH algorithms, by about 7 times for BD, and by 9 times for ChI (at E_b/N_0 = 27 dB). The explicit line of sight (K = 100) increases BER by about 90 times for DPC and TH, by 21 times for BD, and by 32 times for ChI at E_b/N_0 = 27 dB. Only the DPC and TH algorithms allow achieving BER < 0.1 (0.05 and 0.08, respectively). Thus, DPC is most resistant to the presence of line of sight in the channel.

Fig. 5 shows that a weak spatial correlation has almost no effect on noise immunity. Correlation at level $\rho = 0.5$ leads to an increase in BER by about 3–4 times at E_b/N_0 = 27 dB. At $\rho = 0.8$ and E_b/N_0 = 27 dB, BER increases by 128, 101, 32, and 52 times for DPC, TH, BD and ChI, respectively. At the same time, DPC and TH make it possible to achieve BER < 0.1 (0.06 and 0.09, respectively), whereas when using BD and ChI, BER values are 0.2 and 0.5. Consequently, DPC is most resistant to spatial correlation.

As can be seen from Fig. 6, with perfect estimation and NTRF = 8, the noise immunity is lower than that achieved with the ChI algorithm, and with NTRF = 16, the hybrid beamforming approaches the noise immunity performance of DPC, but it is slightly inferior to it. At NTRF = 16, a small estimation error (MSE = 0.001) leads to a significant decrease in noise immunity, BER increases by about 40 times; while at NTRF = 8, such an error leads to a deterioration in noise immunity by about 4 times (at E_b/N_0 =27 dB). At MSE = 0.01, E_b/N_0 = 27 dB; when NTRF = 16, BER ≈ 0.1; and when NTRF = 8, BER exceeds 0.1. With a larger estimation error (MSE = 0.1), BER exceeds 0.1 even when NTRF = 16.

4. CONCLUSIONS

The article considers the influence of transmission channel parameters on the noise immunity of MIMO systems. The obtained results highlight that MIMO shows robust performance with perfect estimation and a wide variety of channels. However, real conditions often deviate significantly from ideal conditions. The presence of noise, partial or complete absence of multipathing, physical proximity of antenna elements can lead to a significant decrease in the performance of multi-antenna systems. For this reason, the work of MIMO

systems in the light of new technologies, such as machine learning, metamaterials, reconfigurable surfaces, is a significant research issue. For example, reconfigurable surfaces can enhance channel diversity, and machine-learning algorithms can improve the accuracy of channel estimation. Additionally, there is a need for further improvement of the existing beamforming algorithms and the development of new ones, especially in the millimeter and terahertz ranges, to mitigate the consequences of the strong signal attenuation. Research in these areas has the potential to become the basis for enhancements in basic characteristics of forthcoming communication systems. In addition, the integration of MU-MIMO systems with existing multiple-access methods, such as [20, 21], will further improve the communication system performance.

REFERENCES

1. Cho YS, Kim J, Yang WY, & Kang CG. *MIMO-OFDM wireless communications with MATLAB*. Hoboken., NJ, USA,Wiley, 2010: 439.
2. Heath RW, Gonzalez-Prelcic N, Rangan S, Roh W, & Sayeed AM. An overview of signal processing techniques for millimeter wave MIMO systems. *IEEE journal of selected topics in signal processing*, 2016, 10(3):436-453.
3. Spencer QH, Swindlehurst AL, & Haardt M. Zero-forcing methods for downlink spatial multiplexing in multiuser MIMO channels. *IEEE transactions on signal processing,* 2004, 52(2):461-471.
4. Peel CB, Hochwald BM, & Swindlehurst AL. A vector-perturbation technique for near-capacity multiantenna multiuser communication-part I: channel inversion and regularization. *IEEE Transactions on Communications*, 2005, 53(1):195-202.
5. Costa M. Writing on dirty paper (corresp.). *IEEE transactions on information theory,* 1983, 29(3):439-441.
6. Fischer RF, Windpassinger C, Lampe A, & Huber JB. Space-time transmission using Tomlinson-Harashima precoding. *ITG FACHBERICHT,* 2002:139-148.
7. Sadek M, Tarighat A, & Sayed, AH. A leakage-based precoding scheme for downlink multi-user MIMO channels. *IEEE transactions on Wireless Communications,* 2007, 6(5):1711-1721.
8. Gao X, Edfors O, Rusek F, & Tufvesson F. Linear pre-coding performance in measured very-large MIMO channels. *Proc. IEEE vehicular technology conference* (*VTC Fall*), 2011:1-5.
9. Heath RW, Gonzalez-Prelcic N, Rangan S, Roh W, & Sayeed AM. An overview of signal processing techniques for millimeter wave MIMO systems. *IEEE journal of selected topics in signal processing*, 2016, 10(3):436-453.
10. Shahramian S, Yasotharan H, & Carusone AC. Decision feedback equalizer architectures with multiple continuous-time infinite impulse response filters. *IEEE Transactions on Circuits and Systems II: Express Briefs,* 2012, 59(6):326-330.
11. Tomlinson, M. New automatic equaliser employing modulo arithmetic. *Electronics letters,* 1971, 7(5):138-139.
12. Harashima H, & Miyakawa H. Matched-transmission technique for channels with intersymbol interference. I*EEE Transactions on Communications*, 1972, 20(4):774-780.
13. Joham M, Utschick W, & Nossek, JA. Linear transmit processing in MIMO communications systems. *IEEE*

Transactions on signal Processing, 2005, 53(8):2700-2712.

14. Molisch AF, Ratnam VV, Han S, Li Z, Nguyen SLH, Li L, & Haneda K. Hybrid beamforming for massive MIMO: A survey. *IEEE Communications magazine*, 2017, 55(9):134-141.
15. Tyrtyshnikov EE. *Matrichnyi analiz i lineynaya algebra* [Matrix analysis and linear algebra.]. Mocsow, Fizmatlit Publ., 2007, 480 p.
16. El Ayach O, Rajagopal S, Abu-Surra S, Pi Z, & Heath RW. Spatially sparse precoding in millimeter wave MIMO systems. *IEEE transactions on wireless communications*, 2014, 13(3):1499-1513.
17. Tropp JA, & Gilbert AC. Signal recovery from random measurements via orthogonal matching pursuit. *IEEE Transactions on information theory*, 2007, 53(12):4655-4666.
18. Yu X, Shen JC, Zhang J, & Letaief, KB. Alternating minimization algorithms for hybrid precoding in millimeter wave MIMO systems. *IEEE Journal of Selected Topics in Signal Processing,* 2016, 10(3):485-500.
19. Zhang J, Yu X, & Letaief KB. Hybrid beamforming for 5G and beyond millimeter-wave systems: A holistic view. *IEEE Open Journal of the Communications Society*, 2019, 1:77-91.
20. Pokamestov DA, Kryukov YV, Rogozhnikov EV, & Kanatbekuli I., Adapting SCMA Codebooks to Channel State. *Proc. 3rd International Youth Conference on Radio Electronics, Electrical and Power Engineering* (*REEPE*), 2021:1-4.
21. Kryukov YV, Pokamestov DA, Rogozhnikov EV, Demidov AY, & Gromova YS. Experimental research of PD/NOMA. *Proc. 19th International Conference of Young Specialists on Micro/Nanotechnologies and Electron Devices* (*EDM*), 2018:176-179.